International Journal of Solids and Structures 50 (2013) 320–327

Contents lists available at SciVerse ScienceDirect

International Journal of Solids and Structures

journal homepage: www.elsevier.com/locate/ijsolstr

A Gurson-type model accounting for void size effects

Vincent Monchiet *, Guy Bonnet

Université Paris-Est, Laboratoire Modélisation et Simulation Multi Echelle, MSME UMR8208 CNRS, 5 Boulevard Descartes, 77454 Marne la Vallée Cedex, France

ARTICLE INFO

Article history:
Received 16 July 2012
Received in revised form 3 September 2012
Available online 13 October 2012

Keywords:
Ductile porous materials
Yield criterion
Gradient plasticity
Void size effect
Limit analysis

ABSTRACT

In this paper we present an extension of the Gurson model of cavity growth which includes the void size effect. To this end, we perform the limit analysis of a hollow sphere made up of a Fleck and Hutchinson's strain gradient plasticity material. Based on the trial velocity field of Gurson, we derive an approximate closed form expression of the macroscopic criterion. The latter incorporates the void size dependency through a non dimensional parameter defined as the ratio of the cavity radius and the intrinsic length of the plastic solid. The accuracy of this approximate criterion is demonstrated by its comparison with numerical data. In the last part of the paper we present a complete plasticity model involving the damage rate and a power-law strain hardening of the matrix. It is shown that the cavity size effect has a strong dependency on damage growth as well as on the stress strain response.

1. Introduction

Micromechanics approaches based on limit analysis have been widely used for the modeling of ductile porous materials since the pioneering works of Rice and Tracey (1969) and Gurson et al. (1977). On its original form, the Gurson model provides the yield surface, the flow rule and the damage growth law for plastic materials containing spherical voids. It is based on the limit analysis of a hollow sphere made up of a von Mises rigid plastic material and subjected to an arbitrary loading. The Gurson model has been largely employed in the literature for the simulation of the macroscopic response of ductiles metals and particularly for the prediction of material failure (see Tvergaard, 1990 and Benzerga and Leblond, 2010 for a review of such applications). Various extensions of the Gurson model have then been provided in order to account for the void shape effects (Gologanu et al., 1993, 1994, SPS Year; Monchiet et al., 2007), the initial plastic anisotropy (Benzerga and Besson, 2001; Monchiet et al., 2008), the matrix compressibility (Jeong, 2002; Monchiet and Kondo, 2012).

However, it is worthwhile noticing that, as already mentioned by Hutchinson (2000): "*Application of void growth prediction based on the conventional plasticity to submicron sized voids is probably unjustified*". Indeed, the plasticity at micron scale displays a strong size dependency, as shown experimentally by micro-twist (Fleck et al., 1994), micro indentation (Nix and Gao, 1998), micro bending (Stolken and Evans, 1998). Note also that experimental studies of Schlueter et al. (1996) and Khraishi et al. (2001), have reported a strong effect of the cavity size on their growth in plastic media. The size effect is interpreted as due to the dependence of the plastic solid with an internal length scale which is physically attributed to the generation and the storage of geometrically necessary dislocations (Nye, 1953; Cottrell, 1964; Ashby et al., 1970; Fleck et al., 1994; Gao et al., 1999). When the size of the cavities is comparable to or smaller than the internal length of the plastic solid, the application of the Gurson model appears to be questionable. This motivated many researchers to investigate the role of the cavity size on the macroscopic behavior of porous plastic materials. Among the first, Fleck and Hutchinson successively employed the couple-stress plasticity theory (Fleck and Hutchinson, 1993) or their more general strain gradient plasticity theory (Fleck and Hutchinson, 1997) to study the growth of an isolated spherical void embedded in an infinite solid. Note that, still in the context of an isolated void and on the basis of the Fleck and Hutchinson strain gradient plasticity model, Li and Huang (2005) has studied the combined effect of void size and void shape by considering the case of a spheroidal cavity. Alternatively, Huang et al. (2000) and Liu et al. (2003, 2005) have studied the growth of an isolated void by considering the Taylor dislocation based strain gradient plasticity theory introduced in Gao et al. (1999). On a general matter, all these studies has reported a strong effect of the cavity size on their growth. More precisely, they found that, at micron scales, the smaller void is more difficult to grow than the larger one. Later, Li et al. (2003) and Wen et al. (2005) respectively employed the Fleck and Hutchinson strain gradient theory and the Taylor dislocation model of Gao et al. (1999) to extend the Gurson model. The studies have reported a strong dependence of the yield locus of porous plastic material with the cavity size. In Li et al. (2003), the authors do not deliver a closed form expression of the macroscopic criterion while in Wen et al.

* Corresponding author.
E-mail addresses: vincent.monchiet@univ-paris-est.fr (V. Monchiet), guy.bonnet@univ-paris-est.fr (G. Bonnet).

0020-7683/$ - see front matter © 2012 Elsevier Ltd. All rights reserved.
http://dx.doi.org/10.1016/j.ijsolstr.2012.09.005

(2005) the criterion takes the form of a parametric integral equation. Note that for various application to the prediction of failure in ductiles metals, it will be greatly appreciated to have a closed form expression of the macroscopic criterion which accounts for the void size effect.

In this paper we propose to derive an analytic model for ductile porous materials containing spherical micro and sub-micron cavities. To reach this objective, we perform, in Section 3, the limit analysis of a hollow sphere made up of a the strain gradient plasticity solid described by the Fleck and Hutchinson's model (Fleck and Hutchinson, 1997) (briefly recalled in the next section). In Section 4, we derive the complete set of equations of a plasticity model including the damage and cavity size growth law and a power-law hardening. As an illustration purpose we simulate the macroscopic response of the porous plastic solid for various macroscopic loading cases and initial cavity sizes.

2. Limit analysis of the hollow sphere accounting for local gradients

The Gurson models are well known for giving the macroscopic yield locus of plastic media containing spherical or cylindrical cavities. The approach is based on the limit analysis of a hollow sphere or cylinder (depicted in Fig. 1) made up of a rigid ideally plastic von Mises material. In order to incorpore the void size effects at the macroscopic scale we consider, for the solid matrix, the Fleck and Hutchinson strain gradient plasticity model (Fleck and Hutchinson, 1997) instead of the von Mises one.

In this section, we briefly recall here the main steps of the methodology followed by Li and Huang, 2005; Li and Steinmann, 2006 for the limit analysis of a unit cell made up of a strain gradient perfectly plastic material.[1] In the next of the paper, we only consider the case of a hollow sphere. The results for the cylindrical void are given in Appendix A. We consider the spherical basis $(\underline{e}_r, \underline{e}_\theta, \underline{e}_\varphi)$ and the associated coordinates system (r, θ, φ), with $\theta \in [0, 2\pi]$ and $\varphi \in [0, \pi]$. A hollow sphere, with an external radius b and a void of radius a, is subjected at its outer boundary to a homogeneous strain rate conditions:

$$\underline{v}(r = b) = \boldsymbol{D} \cdot \underline{x} \tag{1}$$

where $\underline{v}$ is the velocity field and $\boldsymbol{D}$ denotes the macroscopic strain rate tensor. The solid matrix is assumed to obey the strain gradient plasticity model of Fleck and Hutchinson (1997). This non local plasticity law is formulated with the strain rate $\boldsymbol{d}$ and the double gradient of velocity, $\boldsymbol{\eta}$, given by:

$$d_{ij} = \frac{1}{2}(v_{i,j} + v_{j,i}), \quad \eta_{ijk} = v_{k,ij} \tag{2}$$

With the above definitions, the strain rate tensor $\boldsymbol{d}$ is symmetric and the gradient of strain rate, $\boldsymbol{\eta}$, is symmetric according to its two first indices ($\eta_{ijk} = \eta_{jik}$). Due to the incompressibility of the matrix, the strain rate tensor is traceless, $\mathrm{tr}(\boldsymbol{d}) = 0$ while $\eta_{ipp} = 0$. Following Fleck and Hutchinson (1997), the third order tensor $\boldsymbol{\eta}$ can be decomposed into:

$$\boldsymbol{\eta} = \boldsymbol{\eta}^{(1)} + \boldsymbol{\eta}^{(2)} + \boldsymbol{\eta}^{(3)} \tag{3}$$

where the third order tensors $\boldsymbol{\eta}^{(i)}$ for $i = 1, 2, 3$ are defined by:

$$\begin{aligned} \eta^{(1)}_{ijk} &= \tfrac{1}{3}(\eta_{ijk} + \eta_{ikj} + \eta_{jki}) - \tfrac{2}{15}\left[\alpha_i\delta_{jk} + \alpha_j\delta_{ik} + \alpha_k\delta_{ij}\right] \\ \eta^{(2)}_{ijk} &= \tfrac{1}{3}(2\eta_{ijk} - \eta_{ikj} - \eta_{jki}) + \tfrac{1}{6}\left[2\alpha_k\delta_{ij} - \alpha_i\delta_{jk} - \alpha_j\delta_{ik}\right] \\ \eta^{(3)}_{ijk} &= \tfrac{3}{10}\left[\alpha_i\delta_{jk} + \alpha_j\delta_{ik}\right] - \tfrac{1}{5}\alpha_k\delta_{ij} \end{aligned} \tag{4}$$

[1] Li et al. (2003) and Li and Steinmann (2006) have performed the limit analysis in the context of a strain gradient viscoplastic material, the case of the perfectly plastic material considered in this paper corresponds to limit case for which the viscoplastic power-law exponent tends to infinity.

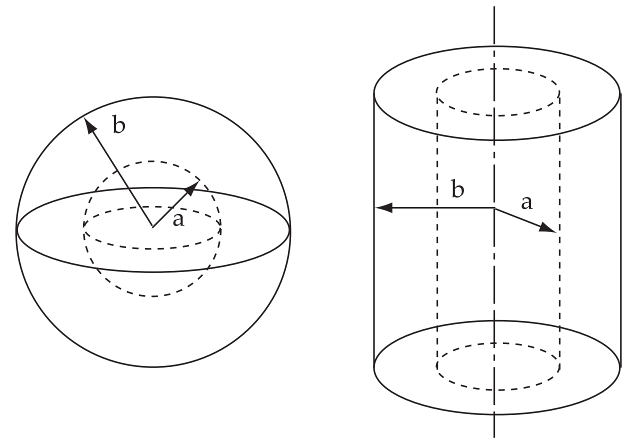

Fig. 1. The hollow sphere and the hollow cylinder.

with:

$$\alpha_i = \eta_{ppi} = v_{i,pp} \tag{5}$$

The local dissipation reads:

$$\pi(\boldsymbol{d}, \boldsymbol{\eta}) = \sigma_0\xi_{eq} = \sigma_0\sqrt{d_{eq}^2 + l_1^2\eta^{(1)}_{ijk}\eta^{(1)}_{ijk} + l_2^2\eta^{(2)}_{ijk}\eta^{(2)}_{ijk} + l_3^2\eta^{(3)}_{ijk}\eta^{(3)}_{ijk}} \tag{6}$$

where d_{eq} is the von Mises equivalent strain rate, $d_{eq} = \sqrt{\frac{2}{3}\boldsymbol{d} : \boldsymbol{d}}$, while l_1, l_2, l_3 are the internal length scales of the material. Experimental investigations (see Fleck et al., 1994; Stolken and Evans, 1998), revealed that the order of magnitude of the constitutive coefficients of strain gradient plastic law, i.e. l_1, l_2, l_3, is generally of the micrometer. In (6), the terms $\eta^{(i)}_{ijk}\eta^{(i)}_{ijk}$ are the three isotropic invariants of the strain rate gradient tensor $\boldsymbol{\eta}$. The modified equivalent strain rate ξ_{eq} defining the local dissipation (6) is the most general isotropic combination of quadratic terms in $\boldsymbol{d}$ and $\boldsymbol{\eta}$.

All invariants are given:

$$\begin{aligned} \eta^{(1)}_{ijk}\eta^{(1)}_{ijk} &= \tfrac{1}{3}(\eta_{ijk}\eta_{ijk} + 2\eta_{ijk}\eta_{kji}) \\ \eta^{(2)}_{ijk}\eta^{(2)}_{ijk} &= \tfrac{2}{3}(\eta_{ijk}\eta_{ijk} - \eta_{ijk}\eta_{kji}) + \alpha_k\alpha_k \\ \eta^{(3)}_{ijk}\eta^{(3)}_{ijk} &= \tfrac{3}{5}\alpha_i\alpha_i \end{aligned} \tag{7}$$

The macroscopic potential is defined by:

$$\Pi(\boldsymbol{D}) = \inf_{\underline{v}^* K.A.}\left[\tfrac{1}{V}\int_{\Omega-\omega}\pi(\boldsymbol{d}, \boldsymbol{\eta})dV\right] \tag{8}$$

for any kinematically admissible (K.A.) velocity field $\underline{v}^*$, complying with the homogeneous strain rate boundary conditions (1). Note first that the consideration of the local strain rate gradient into the definition of the dissipation allows to capture the void size effect for very small cavities. Note also that the macroscopic dissipation is only a function of the macroscopic strain rate tensor. Then, the overall behavior does not exhibit nonlocal effects. The incorporation of the macroscopic strain rate gradient effects on the overall behavior of ductile porous materials could be done by considering higher order type boundary conditions as already done by SPS Name (SPS Year). However these effects do not address the issue of microscopic strain gradient on the growth of cavities, as done in the present paper. As mentioned in Li et al. (2003) and Li and Steinmann (2006), the consideration of the standard homogeneous boundary conditions (1) is justified if the size of the representative volume element (modelized here by the hollow sphere) is very large compared with the internal length scales and the size of the microstructural elements (the cavities). In this configuration, there is a strict separation between the microscopic and macroscopic scales and standard homogenization principles can still be applied.

3. Closed form expression of the macroscopic criterion

We use, for the trial velocity field, the one considered by Gurson:

$$\underline{v}^* = \overline{\boldsymbol{D}} \cdot \underline{x} + \frac{b^3}{r^2} D_m \underline{e}_r \tag{9}$$

where $\overline{\boldsymbol{D}}$ and D_m denote respectively the deviatoric and mean parts of the macroscopic strain rate tensor and are defined by $\overline{\boldsymbol{D}} = \boldsymbol{D} - D_m \boldsymbol{I}$ and $D_m = \mathrm{tr}(\boldsymbol{D})/3$, $\boldsymbol{I}$ being the second order identity tensor. It must be recalled that the trial velocity field (9) complies with the matrix incompressibility and with the uniform strain rate boundary conditions (1). The components of the microscopic strain rate are:

$$d_{ij} = \overline{D}_{ij} + \frac{b^3}{r^3} D_m \left[\delta_{ij} - 3\frac{x_i x_j}{r^2}\right] \tag{10}$$

while the components of the double gradient of the velocity field are given by:

$$\eta_{ijk} = -\frac{3b^3}{r^5} D_m \left[\delta_{ij} x_k + \delta_{ik} x_j + \delta_{jk} x_i - \frac{5}{r^2} x_i x_j x_k\right] \tag{11}$$

For the calculation of the invariants in (7), it is convenient to note that the trial velocity (9) derivates from the harmonic potential Φ given by:

$$\Phi = \frac{1}{2}\overline{D}_{ij} x_i x_j - \frac{b^3}{r} D_m \tag{12}$$

As a consequence, the double gradient of the velocity field reads $\eta_{ijk} = \Psi_{,ijk}$ and is invariant by any permutations of its indices i, j, k. Moreover, Ψ being harmonic, it follows that $\eta_{ijj} = \eta_{jij} = \eta_{jji} = \Psi_{,ijj} = 0$. Vector $\underline{\alpha}$, defined by relation (5), is then null. It can be easily shown from (4) that $\boldsymbol{\eta}^{(2)} = \boldsymbol{\eta}^{(3)} = 0$ and $\boldsymbol{\eta}^{(1)} = \boldsymbol{\eta}$. The macroscopic dissipation, defined by relation (8), reads:

$$\Pi(\boldsymbol{D}) = \frac{3\sigma_0}{b^3} \int_{r=a}^{r=b} \langle \xi_{eq} \rangle_{S(r)} r^2 dr \tag{13}$$

with:

$$\xi_{eq} = \left[D_{eq}^2 - \frac{4b^3}{r^3} D_m \overline{D}_{rr} + \frac{2b^6}{r^6}\left(2 + \frac{45 l_1^2}{r^2}\right) D_m^2\right]^{1/2} \tag{14}$$

and $\langle \bullet \rangle_{S(r)}$ represents the integral over the unit sphere, defined as follows:

$$\langle \bullet \rangle_{S(r)} = \frac{1}{4\pi} \int_{\varphi=0}^{\varphi=\pi} \int_{\theta=0}^{\theta=2\pi} \bullet \sin(\varphi) d\varphi d\theta \tag{15}$$

Note that the main difference with the Gurson analysis lies in the term proportional to l_1^2 in the expression of ξ_{eq}. It is not possible to derive the closed form expression of the integral in (13). Some approximations are then needed in order to obtained an analytic expression of the macroscopic criterion. The first, already used by Gurson himself, is the following:

$\mathcal{A}1$: we replace in (13), the integral $\langle \xi_{eq} \rangle_{S(r)}$ by $[\langle \xi_{eq}^2 \rangle_{S(r)}]^{1/2}$.

This first approximation has the advantage of preserving the upper bound character of the approach. Since the integral of $\overline{D}_{rr}$ over the unit sphere is null, the second term in the expression of ξ_{eq} vanishes and the expression for $\Pi(\boldsymbol{D})$ becomes:

$$\Pi(\boldsymbol{D}) = \frac{3\sigma_0}{b^3} \int_{r=a}^{r=b} \left[D_{eq}^2 + \frac{2b^6}{r^6}\left(2 + \frac{45 l_1^2}{r^2}\right) D_m^2\right]^{1/2} r^2 dr \tag{16}$$

Again, an approximation is needed for computing the integral in the above expression of $\Pi(\boldsymbol{D})$.

$\mathcal{A}2$: We replace the integral in (16) by an integral on the form:

$$\Pi(\boldsymbol{D}) = \frac{3\sigma_0}{b^3} \int_{r=a}^{r=b} \left[D_{eq}^2 + \frac{4\eta^2 b^6}{r^6} D_m^2\right]^{1/2} r^2 dr \tag{17}$$

where coefficient η is a constant which will be given in the following.

The integral in (17) is exactly the one performed by in Gurson et al. (1977) when $\eta = 1$ (more details about its computation can be found in Gurson et al. (1977) or in Leblond (2003)). The closed form of (17) is then easily obtained by using the following appropriate transformation $D_m \to \eta D_m$ in the result of Gurson. This closed form is:

$$\Pi(\boldsymbol{D}) = \sigma_0 \left[2\eta D_m \mathrm{arcsinh}\left(\frac{2\eta D_m}{u D_{eq}}\right) - \sqrt{4\eta^2 D_m^2 + u^2 D_{eq}^2}\right]_{u=1}^{u=f} \tag{18}$$

and leads to the following expression for the macroscopic yield surface:

$$\Phi(\boldsymbol{\Sigma}, f, \eta) = \frac{\Sigma_{eq}^2}{\sigma_0^2} + 2f\cosh\left(\frac{3}{2\eta}\frac{\Sigma_m}{\sigma_0}\right) - 1 - f^2 = 0 \tag{19}$$

We now propose to evaluate coefficient η. It can be found by studying the particular case of a pure hydrostatic loading. Indeed, by putting $D_{eq} = 0$ in (16), one obtains:

$$\Pi(\boldsymbol{D}) = 6\sigma_0 |D_m| \int_{r=a}^{r=b} \left[1 + \frac{45 l_1^2}{2r^2}\right]^{1/2} \frac{dr}{r} \tag{20}$$

by using the change of variable $u = a/r$, the above integral can be put into the form:

$$\Pi(\boldsymbol{D}) = 6\sigma_0 |D_m| \int_{u=f^{1/3}}^{u=1} \left[1 + \frac{u^2}{\alpha^2}\right]^{1/2} \frac{du}{u} \tag{21}$$

with:

$$\alpha = \frac{1}{3}\sqrt{\frac{2}{5}}\frac{a}{l_1} \tag{22}$$

The computation of the integral in (21) gives:

$$\Pi(\boldsymbol{D}) = -6\sigma_0 |D_m| \left[\mathrm{arcsinh}\left(\frac{\alpha}{u}\right) - \sqrt{1 + \frac{u^2}{\alpha^2}}\right]_{u=f^{1/3}}^{u=1} \tag{23}$$

On the other hand, by taking the limit $D_{eq} \to 0$ in the approximate expression of $\Pi(\boldsymbol{D})$, given by (18), one has:

$$\Pi(\boldsymbol{D}) = -2\sigma_0 \eta |D_m| \ln(f) \tag{24}$$

Expressions (24) and (23) are equivalent, by taking the following expression for η:

$$\eta = \frac{3}{\ln(f)} \left[\mathrm{arcsinh}\left(\frac{\alpha}{u}\right) - \sqrt{1 + \frac{u^2}{\alpha^2}}\right]_{u=f^{1/3}}^{u=1} \tag{25}$$

where it is recalled that α is given by (22).

To summarize, the new macroscopic criterion for plastic porous material (19) only differs from the Gurson criterion by the presence of coefficient η within the hyperbolic cosine. This coefficient, given by (25) together with relation (22), introduces the size effect since the non dimensional parameter α depends on the cavity radius a. When a is large behind the intrinsic length l_1, coefficient α takes also large values and coefficient η tends to 1. So, in this case, one recovers the yield surface given by the Gurson model (Gurson et al., 1977). It must be emphasized that the macroscopic yield surface has no dependence from the two other constitutives coefficients l_2 and l_3 which enter the strain gradient plasticity model of Fleck and Hutchinson (1997). The reason is mainly due to the choice of the trial velocity field used to perform the limit analysis of the hollow sphere. This field is the one already considered by Gurson and it has the property (as already mentioned in the text) to derivate form an harmonic potential. This has the consequence that the two isotropic invariants $\eta_{ijk}^{(2)}\eta_{ijk}^{(2)}$ and $\eta_{ijk}^{(3)}\eta_{ijk}^{(3)}$, in the expression of the dissipation, are null and the latter is then not affected by the material parameters l_2 and l_3. In fact, by choosing the trial field considered by Gurson, the expression of the strain gradient only depends on the hydrostatic strain rate, D_m. So, the considered field cannot account for the strain gradients which will occur at the vicinity of the void when the cell is submitted to a macroscopic shear strain loading. In fact, a possible way to investigate the role of this strain gradients and the parameters l_2 and l_3 on the macroscopic criterion is to consider more refined velocity fields as already done in Monchiet et al. (2011).

Our model requires the knowledge of coefficient l_1. From a more general point of view, experimental studies showed that for most metallic materials, coefficients l_1, l_2 and l_3 are given by (see Begley and Hutchinson, 1998 or Hutchinson, 2000):

$$l_1 = l_{SG}, \quad l_2 = \frac{l_{RG}}{2}, \quad l_3 = \sqrt{\frac{5}{24}} l_{RG} \tag{26}$$

values for which, the modified equivalent strain can be put into the form:

$$\xi_{eq} = \sqrt{d_{eq}^2 + l_{SG}^2 \eta_{ijk}^{(1)} \eta_{ijk}^{(1)} + \frac{2}{3} l_{RG}^2 \chi_{ij} \chi_{ij}} \tag{27}$$

where χ_{ij} is the gradient of rotation. The case $l_{SG} = 0$ corresponds to the particular case of the couple stress plasticity theory of Fleck and Hutchinson (1993) while for $l_{SG} = l_{RG} = 1$ the material depends on both stretch and gradient of rotation. In the particular case of the couple stress theory, one has $l_1 = 0$, while the non dimensional parameter α tends to infinity and $\eta = 1$. Therefore, the porous plastic material does not exhibit a void size dependency when the matrix is described by the couple stress plasticity theory of Fleck and Hutchinson (1993). Based on various available experimental data, Hutchinson (2000) has concluded that the characteristic length l_{SG} lies between 0.25 and 1 μm, while $l_{RG} \simeq 1$ μm. For the different applications proposed in this section and also in the next section, we considered $l_{SG} = 0.5$ μm.

The derivation of a closed-form expression of the macroscopic criterion (19) has required two approximations ($\mathcal{A}1$ and $\mathcal{A}2$). As already mentioned, the first one preserves the upper bound character of the approach; however, the second one ($\mathcal{A}2$) is "uncontrolled". However, it will be shown now that these approximations do not alter significantly the macroscopic criterion. In order to validate our criterion, we propose to check its accuracy by comparison with the criterion obtained by computing numerically the integrals in (13). In Figs. 2 and 3 we represent the macroscopic criterion for the porosities $f = 0.01$ and $f = 0.1$ respectively and for various values of the void radius a. For comparison purpose we also represent the Gurson criterion on each figure. The full line corresponds to the approximate criterion given by Eq. (19) together with the definition (25) for coefficient η. The circles correspond to the criterion obtained by computing numerically the macroscopic dissipation with the trial velocity field (9). A good agreement between the approximate and numerical criterion is observed for all values of the porosity and of the size of the cavities. The results show an important effect of the cavity radius a on the macroscopic yield locus: the yield strength domain increases when the void size decreases. These effects are particularly important for high stress triaxiality $T = \Sigma_m/\Sigma_{eq}$. However, for purely deviatoric loading cases ($\Sigma_m = 0$) the void size does not affect the yield stress for which the new criterion (19) retrieves the Gurson one. It must be emphasized that the present results differ from the one provided by Wen et al. (2005). Indeed, the results obtained by Wen et al. (2005) exhibit an increase of the yield stress when decreasing the void size effect for purely deviatoric loadings, which is not observed in the present study. These differences can be attributed to the considered strain gradient plasticity model for the solid matrix. Indeed, Wen et al. (2005) used the Taylor dislocation based strain gradient plasticity model of Gao et al. (1999) instead of the Fleck and Hutchinson model (Fleck and Hutchinson, 1997) considered in this paper.

4. Plastic model accounting for void size

In order to complete the set of equations for the ductile porous metal, we now provide the evolution law for the plastic strain, the porosity and the cavity size.

The criterion (19) has been established in the context of perfect plasticity. The model derived from this criterion will not account for elasticity deformation and plastic strain hardening. To circumvent these incapacities, we follow the heuristical extension of Gurson et al. (1977), widely used in the literature (see for instance Tvergaard, 1990; Benzerga and Leblond, 2010). Along the lines of these authors, the total strain rate is written as the sum of an elastic part $\boldsymbol{D}^e$ and a plastic part $\boldsymbol{D}^p$. Here the elastic part $\boldsymbol{D}^e$ is related to the macroscopic stress-rate $\dot{\boldsymbol{\Sigma}}$ by Hooke's law. In order to account for the plastic strain hardening, the yield stress σ_0 is replaced by $\tau(p)$ where p is the cumulated plastic strain which is identified from the following plastic dissipation identity:

$$(1-f)\tau(p)\dot{p} = \boldsymbol{\Sigma} : \boldsymbol{D}^p \tag{28}$$

Other various heuristical modifications of the original Gurson model have been also proposed, in order to take into account void interaction or void coalescence (see Tvergaard, 1982; Tvergaard and Needleman, 1984), but they are not considered in this paper. With the definition of the macroscopic criterion $\Phi(\boldsymbol{\Sigma}, f, \eta)$ given by (19), the flow rule is:

$$\begin{cases} \overline{\boldsymbol{D}}^p = \Lambda \frac{\partial \Phi}{\partial \overline{\boldsymbol{\Sigma}}} = \Lambda \frac{3\overline{\boldsymbol{\Sigma}}}{\tau^2} \\ D_m^p = \Lambda \frac{1}{3} \frac{\partial \Phi}{\partial \Sigma_m} = \Lambda \frac{f}{\eta \tau} \sinh\left(\frac{3}{2\eta} \frac{\Sigma_m}{\tau}\right) \end{cases} \tag{29}$$

where Λ, the plastic multiplier, has to be determined from the consistency condition $\dot{\Phi} = 0$ (the details of its calculation can be found in Appendix B). Taking into account the incompressibility of the matrix, the porosity evolution law which characterizes the damage growth, takes the form:

$$\dot{f} = 3(1-f) D_m^p \tag{30}$$

The new criterion (19) also depends on the cavity radius through the parameter η which is defined by (25). For completing the model, it is also necessary to derive the rate law of η:

$$\dot{\eta} = -\frac{\eta}{f \ln(f)} \dot{f} + \frac{1}{f \ln(f)} \left[\sqrt{1 + \frac{f^{2/3}}{\alpha^2}} \right] \dot{f} + \frac{3}{\alpha \ln(f)} \left[\sqrt{1 + \frac{u^2}{\alpha^2}} \right]_{u=f^{1/3}}^{u=1} \dot{\alpha} \tag{31}$$

in which the rate law of α is:

$$\dot{\alpha} = \sqrt{\frac{2}{45}} \frac{\dot{a}}{l_1} = \alpha \frac{\dot{a}}{a} \tag{32}$$

Due to the matrix incompressibility, it is possible to connect the cavity growth to the damage growth. Then denoting by ω the volume of the cavity and Ω the total volume of the porous solid, the matrix incompressibility is $\dot{\omega} = \dot{\Omega}$. In the other hand:

$$\dot{f} = \frac{\dot{\omega}}{\Omega} - \frac{\omega}{\Omega^2} \dot{\Omega} = f(1-f) \frac{\dot{\omega}}{\omega} = 3f(1-f) \frac{\dot{a}}{a} \tag{33}$$

Accounting for the above result in relation (32), one obtains:

$$\dot{\alpha} = \frac{\alpha}{3f(1-f)} \dot{f} = \frac{\alpha}{f} D_m^p \tag{34}$$

Eliminating $\dot{\alpha}$ in (31), leads to:

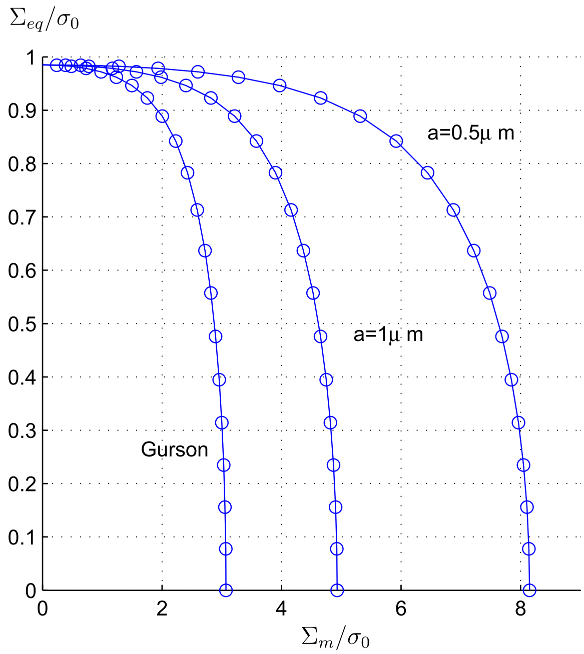

Fig. 2. Macroscopic yield surface for the porosity $f = 0.01$ and for $a_0 = 0.5$ μm, $a_0 = 1$ μm and $a_0 \gg l_{SG}$ (Gurson).

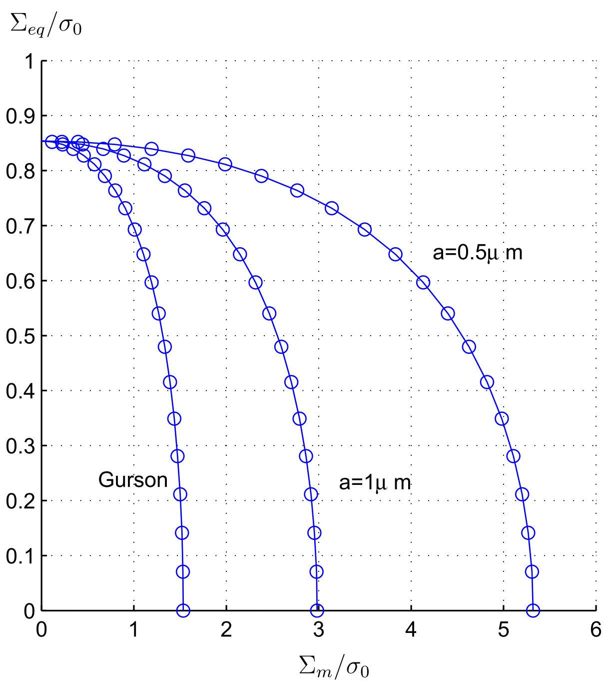

Fig. 3. Macroscopic yield surface for the porosity $f = 0.1$ and for $a_0 = 0.5$ μm, $a_0 = 1$ μm and $a_0 \gg l_{SG}$ (Gurson).

$$\dot{\eta} = \frac{3}{f\ln(f)}\left[\sqrt{1+\frac{1}{\alpha^2}} - f\sqrt{1+\frac{f^{2/3}}{\alpha^2}} - (1-f)\eta\right] D_m^p \tag{35}$$

Relations (30) and (35) give the rate law for the two internal variables which appears in the expression of the macroscopic criterion (19). As an illustration purpose, we propose to simulate the stress strain response for an axisymmetric loading case. The non zero components of the macroscopic stress tensor are:

$$\Sigma_{11} = \Sigma_m - \frac{1}{3}\Sigma_{eq} = \frac{3T-1}{3}\Sigma_{eq}, \quad \Sigma_{33} = \Sigma_m + \frac{2}{3}\Sigma_{eq} = \frac{3T+2}{3}\Sigma_{eq} \tag{36}$$

where it is recalled that $T = \Sigma_m/\Sigma_{eq}$. For the proposed application, we assume that $\Sigma_{33} > \Sigma_{11}$ since $\Sigma_{eq} = \Sigma_{33} - \Sigma_{11}$. By fixing the stress triaxiality T the material is subjected to a radial stress loading in the plane (Σ_{eq}, Σ_m). The stress loading path can then be parameterized by the equivalent stress Σ_{eq}. A power law type hardening law for the matrix material is considered:

$$\tau(p) = \sigma_0\left(1 + \frac{p}{p_0}\right)^n \tag{37}$$

with $p_0 = \sigma_0/E$, E being the Young modulus of the matrix and n the strain hardening exponent. In our calculation, we use the values $E = 200,000$ MPa, $\sigma_0 = 400$ MPa and $n = 0.1$. Furthermore the value $\nu = 0.3$ has been considered for the Poisson's coefficient, the initial porosity being $f_0 = 0.001$. In Fig. 4 we represent the stress–strain response for a triaxiality $T = 1$ for the Gurson model and for the new model accounting for the void size effects. For the latter, the following various values of the initial cavity radius has been considered: $a_0 = 0.1$ μm, $a_0 = 0.5$ μm and $a_0 = 1$ μm. On this figure it is observed that all curves are very close; the void size effect is then not prominent for this value of stress triaxiality. Fig. 5 shows the values of porosity f for the Gurson model and for various initial void radius still for the case of triaxiality $T = 1$. It is observed that the void size has a great influence on damage growth. In Figs. 6 and 7 we display similar results for the triaxiality $T = 3$. Comparatively to the case $T = 1$, the void size effect is prominent on the macroscopic stress strain response which predicts an important reduction of softening (for $a_0 = 1$ μm and $a_0 = 0.5$ μm) or an absence of softening (for $a_0 = 0.1$ μm). Fig. 7 also exhibits a great influence of the cavity size. More generally, for both values of triaxiality, it is noted that the growth rate of smaller cavities is slower than that of larger ones. This result is in agreement with the numerical studies of Fleck et al. (1994), Fleck and Hutchinson (1997), Li et al. (2003), and Li and Steinmann (2006). Physically, this reduction of rate of growth can be explained by the presence of a strong strain gradient which makes the material more hardened at the vicinity of the cavity. Note that an alternative method for incorporating the void size effects in the Gurson limit analysis approach has been recently developed by Dormieux and Kondo (2010). Void size effects are captured by considering at the interface between the matrix and the cavity a plastic version of Gurtin and Murdoch (1975) surface stress model which relates the jump of the traction vector to the interfacial residual stress and interfacial plastic strain rate. This interface tends to account for the thin shell of hardened solid which surrounds the cavity. Interestingly, the results obtained in Dormieux and Kondo (2010) are comparable with those predict by Wen et al. (2005): an increase of the elastic domain for any value of stress triaxiality. However, the flow rule, the damage and cavity radius rate law have not been derived in Dormieux and Kondo (2010) and are then lacking for a full comparison of the models. Note also that the full validation of the present model can be made by computing numerically the solution of the cell problem for the considered boundary conditions. Such kind of results has been provided by Trillat and Pastor (2005) in the context of a von Mises matrix and would need an extension in the case of a strain gradient plastic matrix.

5. Conclusion

This paper has dealt with a micromechanical based modification of the Gurson criterion incorporating the void size effect. The latter is captured within the standard Gurson's limit analysis approach by considering, for the solid matrix, the Fleck and Hutchinson's strain gradient plasticity model (Fleck and Hutchinson, 1997). A closed form approximate expression of the macroscopic yield surface has been derived and assessed through its comparison with numerical data. The results have shown an increase of the yield stress for smaller cavities which is particularly pronounced for high values of stress triaxiality. For larger values of the cavity radius, the new criterion coincides with the one of Gurson.

In a second part of the paper, we provide the damage and void size rate law, incorporating a power-law strain hardening of the solid matrix. The stress–strain response of the ductile porous material containing micro and sub-micron cavities has been simulated for two radial stress loading paths. Those results have shown a strong dependence of void size effects which can be summarized as follows: (i) for smaller cavities the stress and strain response show a reduction or an absence of softening which is observed for the Gurson model and (ii) the smaller cavities growth slower than larger voids. These results, already reported by various numerical studies in the literature (see Fleck and Hutchinson, 1997; Li et al., 2003; Li and Steinmann, 2006) are well reproduced here by our analytic micromechanical-based model. Note that the main feature of the present study is to deliver a closed form expression of the macroscopic plastic criterion as well as the rate law for the internal variables. This is greatly appreciated in the scope of many applications to structural design.

Appendix A. Macroscopic yield criterion for cylindrical cavities

In this section we perform the limit analysis of the hollow cylinder made up of a rigid strain gradient plastic material. We follow the same methodology as the one depicted in Section 3 devoted to the case of a hollow sphere. Since many calculations are similar to that already provided for the hollow sphere, we do not detailed some calculations.

We denote by a the radius of the cavity and by b the external radius. We use the cylindrical coordinate system (ρ, θ, z) and the associated basis $(\underline{e}_\rho, \underline{e}_\theta, \underline{e}_z)$. The homogeneous strain rate boundary condition (1) is considered on the external surface $r = b$. The velocity field used by Gurson et al. (1977) is also considered here (see also Leblond et al., 1994):

$$\underline{v} = \boldsymbol{A} \cdot \underline{x} + \frac{3}{2} D_m \frac{b^2}{\rho} \underline{e}_\rho \tag{A.1}$$

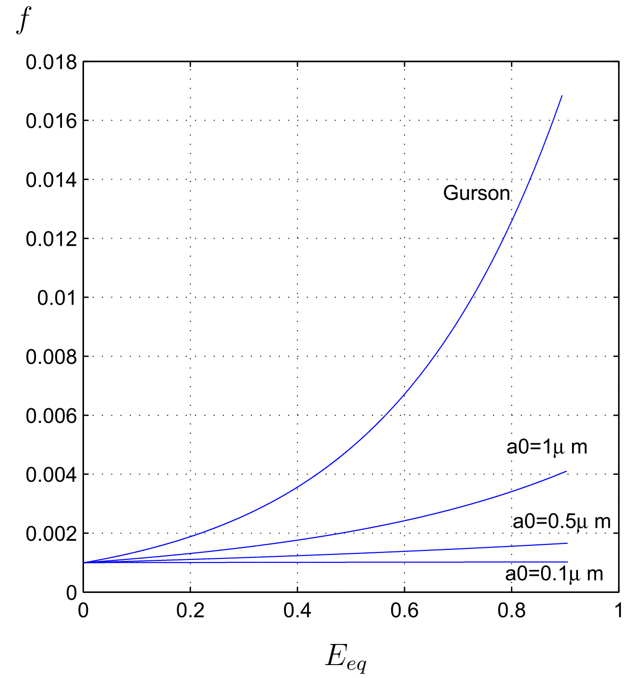

Fig. 5. Porosity vs. the effective strain for various values of the initial cavity size and the Gurson model. Case of a triaxiality $T = 1$.

with:

$$\boldsymbol{A} = \boldsymbol{D} - \frac{3}{2} D_m \boldsymbol{I}_2 \tag{A.2}$$

in which $\boldsymbol{I}_2 = \underline{e}_1 \otimes \underline{e}_1 + \underline{e}_2 \otimes \underline{e}_2 = \underline{e}_\rho \otimes \underline{e}_\rho + \underline{e}_\theta \otimes \underline{e}_\theta$ and it is recalled that $D_m = \mathrm{tr}(\boldsymbol{D})/3$. As for the case of the spherical cavity, the above velocity derivates from an harmonic potential Ψ given by:

$$\Psi = \frac{1}{2} A_{ij} x_i x_j + \frac{3}{2} D_m b^2 \ln(\rho) \tag{A.3}$$

The components of the microscopic strain rate are:

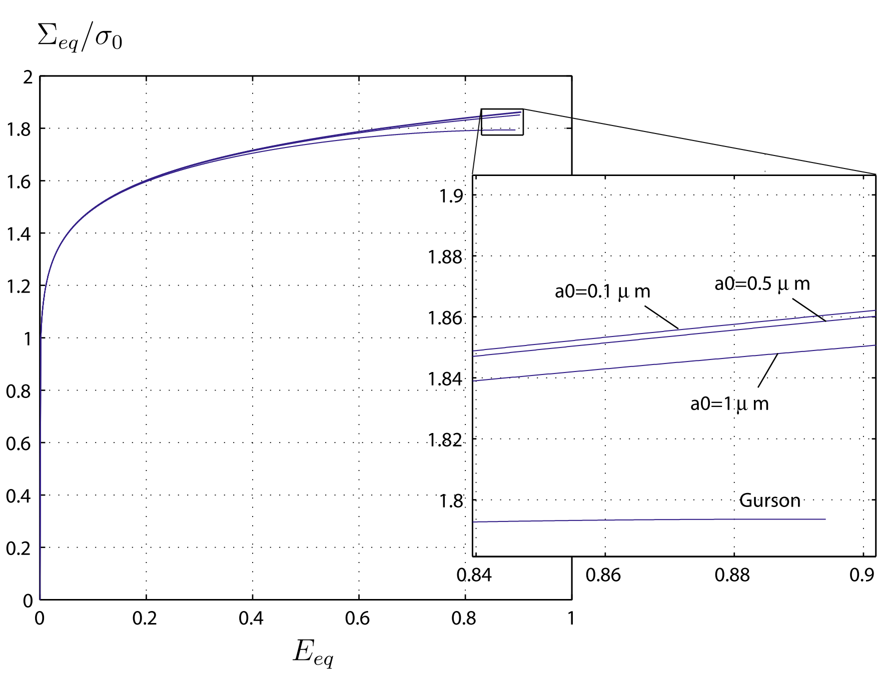

Fig. 4. Normalized equivalent stress vs. the effective strain for various values of the initial cavity size and the Gurson model. Case of a triaxiality $T = 1$.

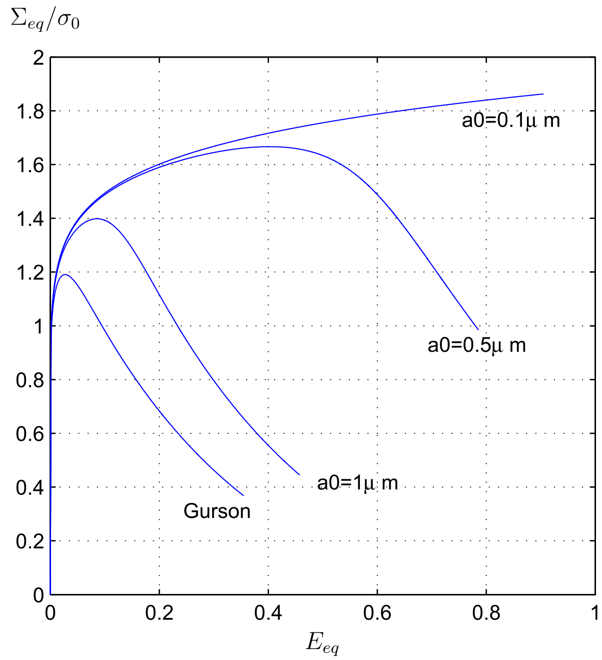

Fig. 6. Normalized equivalent stress vs. the effective strain for various values of the initial cavity size and the Gurson model. Case of a triaxiality $T = 3$.

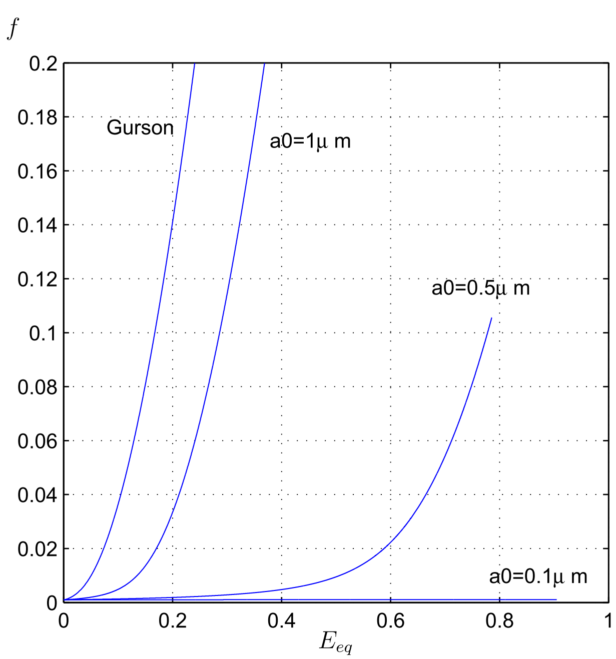

Fig. 7. Porosity vs. the effective strain for various values the initial cavity size and the Gurson model. Case of a triaxiality $T = 3$.

$$d_{ij} = \Psi_{,ij} = A_{ij} - \frac{3D_m}{2}\frac{b^2}{\rho^2}k_{ij} + 3D_m\frac{b^2}{\rho^4}y_i y_j \tag{A.4}$$

where k_{ij} are the components of the second order tensor $\boldsymbol{I}_2$ and $y_i = x_i - x_3\delta_{i3}$. The components of the double gradient of the velocity field are given by:

$$\eta_{ijk} = \Psi_{,ijk} = -3D_m\frac{b^2}{\rho^4}(k_{ij}y_k + k_{ik}y_j + k_{jk}y_i) + 12D_m\frac{b^2}{\rho^6}y_i y_j y_k \tag{A.5}$$

As for the case of the hollow sphere, the double gradient of velocity is invariant by any permutations of its indices i,j,k and $\eta_{iij} = \eta_{jii} = \eta_{jji} = 0$. It follows that $\boldsymbol{\eta}^{(2)} = \boldsymbol{\eta}^{(3)} = 0$ and $\boldsymbol{\eta}^{(1)} = \boldsymbol{\eta}$. The macroscopic dissipation, defined by relation (8), reads:

$$\Pi(\boldsymbol{D}) = \frac{2\sigma_0}{b^2}\int_{\rho=a}^{\rho=b}\langle\xi_{eq}\rangle_{C(\rho)}\rho d\rho \tag{A.6}$$

with:

$$\xi_{eq} = \left[A_{eq}^2 - \frac{3b^2}{\rho^2}D_m\boldsymbol{A}:\boldsymbol{H}(\theta) + \frac{3b^4}{\rho^4}\left(1 + \frac{12l_1^2}{\rho^2}\right)D_m^2\right]^{1/2} \tag{A.7}$$

in which the second order tensor $\boldsymbol{H}(\theta)$ is defined by:

$$\boldsymbol{H}(\theta) = \boldsymbol{I}_2 - \underline{e}_\rho \otimes \underline{e}_\rho \tag{A.8}$$

and $\langle\bullet\rangle_{C(\rho)}$ represents the integral over the unit circle, defined as follows:

$$\langle\bullet\rangle_{C(\rho)} = \frac{1}{2\pi}\int_{\theta=0}^{\theta=2\pi}\bullet d\theta \tag{A.9}$$

We replace in (A.6), the integral $\langle\xi_{eq}\rangle_{C(\rho)}$ by $[\langle\xi_{eq}^2\rangle_{C(\rho)}]^{1/2}$. Since $\langle\boldsymbol{H}(\theta)\rangle_{C(\rho)} = 0$, the crossed term in (A.7) vanishes. The expression of the macroscopic dissipation then becomes:

$$\Pi(\boldsymbol{D}) = \frac{2\sigma_0}{b^2}\int_{\rho=a}^{\rho=b}\left[A_{eq}^2 + \frac{3b^4}{\rho^4}\left(1 + \frac{12l_1^2}{\rho^2}\right)D_m^2\right]^{1/2}\rho d\rho \tag{A.10}$$

As for the case of a spherical cavity, no analytic expression of the above integral can be found. We then replace it by:

$$\Pi(\boldsymbol{D}) = \frac{2\sigma_0}{b^2}\int_{\rho=a}^{\rho=b}\left[A_{eq}^2 + \frac{3\zeta^2 b^4}{\rho^4}D_m^2\right]^{1/2}\rho d\rho \tag{A.11}$$

which has the following expression:

$$\Pi(\boldsymbol{D}) = \sigma_0\left[\sqrt{3}\zeta D_m \operatorname{arcsinh}\left(\frac{\sqrt{3}\zeta D_m}{uA_{eq}}\right) - \sqrt{3\zeta^2 D_m^2 + u^2 A_{eq}^2}\right]_{u=1}^{u=f} \tag{A.12}$$

and leads to the following expression for the macroscopic yield surface:

$$\Phi(\boldsymbol{\Sigma}, f, \zeta) = \frac{\Sigma_{eq}^2}{\sigma_0^2} + 2f\cosh\left(\frac{\sqrt{3}}{2\zeta}\frac{\Sigma_{11} + \Sigma_{22}}{\sigma_0}\right) - 1 - f^2 = 0 \tag{A.13}$$

The same procedure is employed for evaluating coefficient ζ. First, by integrating the macroscopic dissipation (A.11), for $A_{eq} = 0$, we obtain:

$$\Pi(\boldsymbol{D}) = -\sigma_0\sqrt{3}\zeta|D_m|\ln(f) \tag{A.14}$$

On the other hand, the calculation of (A.10) for $A_{eq} = 0$ gives:

$$\begin{aligned}\Pi(\boldsymbol{D}) &= 2\sqrt{3}\sigma_0|D_m|\int_{u=\sqrt{f}}^{u=1}\left[1 + \frac{u^2}{\beta^2}\right]^{1/2}\frac{du}{u}\\ &= -2\sqrt{3}\sigma_0|D_m|\left[\operatorname{arcsinh}\left(\frac{\beta}{u}\right) - \sqrt{1 + \frac{u^2}{\beta^2}}\right]_{u=\sqrt{f}}^{u=1}\end{aligned} \tag{A.15}$$

with:

$$\beta = \frac{1}{2\sqrt{3}}\frac{a}{l_1} \tag{A.16}$$

Expressions (A.14) and (A.15) are equivalent, by taking the following expression for ζ:

$$\zeta = \frac{2}{\ln(f)}\left[\operatorname{arcsinh}\left(\frac{\beta}{u}\right) - \sqrt{1 + \frac{u^2}{\beta^2}}\right]_{u=\sqrt{f}}^{u=1} \tag{A.17}$$

Appendix B. Expression of the plastic multiplier

The Hooke's hypoelastic law gives:

$$\dot{\boldsymbol{\Sigma}} = \mathbb{C} : \boldsymbol{D}^e, \quad \text{with} : \mathbb{C} = 3k\mathbb{J} + 2\mu\mathbb{K} \tag{B.1}$$

where k and μ are respectively the compressibility and shear modulus, $\mathbb{J} = \boldsymbol{I} \otimes \boldsymbol{I}/3$, $\mathbb{K} = \mathbb{I} - \mathbb{J}$ where $\mathbb{I}$ is the fourth order identity tensor. The consistency condition $\dot{\Phi} = 0$ reads:

$$\Phi_{,\boldsymbol{\Sigma}} : \dot{\boldsymbol{\Sigma}} + \left[\Phi_{,\tau} A_\tau + \Phi_{,\alpha} A_\alpha + \Phi_{,f} A_f\right]\Lambda = 0 \tag{B.2}$$

with:

$$\begin{aligned} A_\tau &= \tfrac{1}{\tau}\tfrac{d\tau}{dp}\boldsymbol{\Sigma} : \Phi_{,\boldsymbol{\Sigma}} \\ A_f &= (1-f)\Phi_{,\Sigma_m} \\ A_\eta &= \tfrac{3}{f\ln(f)}\left[\sqrt{1+\tfrac{1}{\alpha^2}} - f\sqrt{1+\tfrac{f^{2/3}}{\alpha^2}} - (1-f)\eta\right]\Phi_{,\Sigma_m} \end{aligned} \tag{B.3}$$

It follows that:

$$\Lambda = \frac{1}{H_\Sigma}\Phi_{,\boldsymbol{\Sigma}} : \dot{\boldsymbol{\Sigma}}, \quad H_\Sigma = \Phi_{,\tau} A_\tau + \Phi_{,\alpha} A_\alpha + \Phi_{,f} A_f \tag{B.4}$$

Due to the equality:

$$\dot{\boldsymbol{\Sigma}} = \mathbb{C} : (\boldsymbol{D} - \boldsymbol{D}^p) = \mathbb{C} : \boldsymbol{D} - \Lambda\mathbb{C} : \Phi_{,\boldsymbol{\Sigma}} \tag{B.5}$$

it is possible to express the plastic multiplier Λ as function of $\boldsymbol{D}$:

$$\Lambda = \frac{1}{H_D}\Phi_{,\boldsymbol{\Sigma}} : \mathbb{C} : \boldsymbol{D}, \quad H_D = H_\Sigma + \Phi_{,\boldsymbol{\Sigma}} : \mathbb{C} : \Phi_{,\boldsymbol{\Sigma}} \tag{B.6}$$

References

Ashby, M.F., 1970. The deformation of plastically non-homogeneous alloys. Philos. Mag. 21, 399–424.
Begley, M.R., Hutchinson, J.W., 1998. The mechanics of size-dependent indentation. J. Mech. Phys. Solids 46, 2049–2068.
Benzerga, A., Besson, J., 2001. Plastic potentials for anisotropic porous solids. Eur. J. Mech. A/Solids 20, 397–434.
Benzerga, A., Leblond, J.B., 2010. Ductile fracture by void growth to coalescence. Adv. Appl. Mech. 44, 169–305.
Cottrell, A.H., 1964. The Mechanical Properties of Matter. John wiley & sons, New York.
Dormieux, L., Kondo, D., 2010. An extension of Gurson model incorporating stresses effects. Int. J. Eng. Sci. 48, 575–581.
Fleck, N.A., Hutchinson, J.W., 1993. A phenomenological theory for strain gradient effects in plasticity. J. Mech. Phys. Solids 41 (12), 1825–1857.
Fleck, N.A., Hutchinson, J.W., 1997. Strain gradient plasticity. Adv. Appl. Mech. 33, 295–361.
Fleck, N.A., Muller, G.M., Ashby, M.F., Hutchinson, J.W., 1994. Strain gradient plasticity: theory and experiment. Acta Metall. Mater. 42 (2), 475–487.
Gao, H., Huang, Y., Nix, W.D., 1999. Modeling plasticity at the micrometer scale. Naturwissenschaften 86, 507–515.
Gologanu, M., Leblond, J.-B., Devaux, J., 1993. Approximate models for ductile metals containing non-spherical voids – case of axisymmetric prolate ellipsoidal cavities. J. Mech. Phys. Solids 41 (11), 1723–1754.
Gologanu, M., Leblond, G., Devaux, J., 1994. Approximate models for ductile metals containing non-spherical voids – case of axisymmetric oblate ellipsoidal cavities. J. Eng. Mater. Technol. 116, 290–297.
Gologanu, M., Leblond, J.B., Perrin, G., Devaux, J., 1997. Recent extensions of Gurson's model for porous ductile metals.In: Suquet, P. (Ed.), Continuum Micromechanics, CISM Courses and lectures nř377. Springer, New York.
Gurson, A.L., 1977. Continuum theory of ductile rupture by void nucleation growth. Part I. – Yield criterion flow rules for porous ductile media. J. Eng. Mater. Technol. 99, 2–15.
Gurtin, M.E., Murdoch, A.I., 1975. A continuum theory of elastic material surfaces. Arch. Ration. Mech. Anal. 57, 291–323.
Huang, Y., Gao, H., Nix, W.D., Hutchinson, J.W., 2000. Mechanism-based strain gradient plasticity II. Analysis. J. Mech. Phys. Solids 48, 99–128.
Hutchinson, J.W., 2000. Plasticity at the micron scale. Int. J. Solids Struct. 37, 225–238.
Jeong, H.-Y., 2002. A new yield function and a hydrostatic stress-controlled model for porous solids with pressure-sensitive matrices. Int. J. Solids Struct. 39, 1385–1403.
Khraishi, T.A., Khaleel, M.A., Zbib, H.M., 2001. Parametric-experimental study of void growth in superplastic deformation. Int. J. Plast. 17, 297–315.
Leblond, J.B., 2003. Mécanique de la rupture fragile et ductile. Hermès Science.
Leblond, J.B., Perrin, G., Suquet, P., 1994. Exact results and approximate models for porous viscoplastic solids. Int. J. Plast. 10, 213–235.
Li, Z., Huang, M., 2005. Combined effects of void shape and void size – oblate spheroidal microvoid embedded in infinite non-linear solid. Int. J. Plast. 21 (3), 625–650.
Li, Z., Huang, M., Wang, C., 2003. Scale-dependent plasticity of porous materials and void growth. Int. J. Solids Struct. 40, 3935–3954.
Li, Z., Steinmann, P., 2006. Rve-based studies on the coupled effects of void size and void shape on yield behavior and void growth at micron scales. Int. J. Plast. 22 (7), 1195–1216.
Liu, B., Qiu, X., Huang, Y., Hwang, K.C., Li, M., Liu, C., 2003. The size effect on void growth in ductile materials. J. Mech. Phys. Solids 51, 1171–1187.
Liu, B., Li, M., Huang, Y., Hwang, K.C., Liu, C., 2005. A study of the void size effect based on the Taylor dislocation model. Int. J. Plast. 21 (11), 2107–2122.
Monchiet, V., Cazacu, O., Charkaluk, E., Kondo, D., 2008. Approximate criteria for anisotropic metals containing non spherical voids. Int. J. Plast. 24, 1158–1189.
Monchiet, V., Charkaluk, E., Kondo, D., 2007. An improvement of Gurson-type models of porous materials by using Eshelby-like trial velocity fields. C.R. Méca. 335 (1), 32–41.
Monchiet, V., Charkaluk, E., Kondo, D., 2011. A micromechanics-based modification of the Gurson criterion by using Eshelby-like velocity fields. Eur. J. Mech. A/Solids 30, 940–949.
Monchiet, V., Kondo, D., 2012. Exact solution of a plastic hollow sphere with a Mises–Schleicher matrix. Int. J. Eng. Sci. 51, 168–178.
Nix, W.D., Gao, H., 1998. Indentation size effects in crystalline materials: a law for strain gradient plasticity. J. Mech. Phys. Solids 46, 411–425.
Nye, J.F., 1953. Some geometrical relations in dislocated crystals. Acta Metall. 1, 153–162.
Rice, J.R., Tracey, D.M., 1969. On a ductile enlargement of voids in triaxial stress fields. J. Mech. Phys. Solids 17, 201–217.
Schlueter, N., Grimpe, F., Bleck, W., Dahl, W., 1996. Modeling of the damage in ductile steels. Comput. Mater. Sci. 7, 27–33.
Stolken, J.S., Evans, A.G., 1998. A microbend test method for measuring the plasticity length scale. Acta Mater. 46, 5109–5115.
Trillat, M., Pastor, J., 2005. Limit analysis and Gurson's model. Eur. J. Mech. A/Solids 24, 800–819.
Tvergaard, V., 1982. On localization in ductile materials containing spherical voids. Int. J. Fract. 18, 237–252.
Tvergaard, V., 1990. Material failure by void growth to coalescence. Adv. Appl. Mech. 27, 83–151.
Tvergaard, V., Needleman, A., 1984. Analysis of cup-cone fracture in round tensile bar. Acta Metall. 32, 157–169.
Wen, J., Huang, Y., Hwang, K.C., Liu, C., Li, M., 2005. The modified Gurson model accounting for the void size effect. Int. J. Plast. 21 (2), 381–395.